Journal of the Korean Nuclear Society
Volume 29, Number 3, pp. 240~250, June 1997

A Study on the Development of Advanced Model to Predict the Sodium Pool Fire

Yong Bum Lee and Seok Ki Choi
Korea Atomic Energy Research Institute
150 Dukjin-dong, Yusong-gu, Taejon 305-353, Korea

(Received September 21, 1996)

Abstract

Liquid sodium is widely used as a coolant of LMR(Liquid Metal Reactor) because of its physical and nuclear properties. However, the liquid sodium is very chemically reactive with oxygen and water so that the study on the sodium fire plays an important role in the LMR safety analysis.

In this study, a sodium fire model is suggested to analyze the sodium pool fire where both the flame and the reaction products are considered. And also, sodium pool fire analysis computer code, SOPA, is developed. The sensitivity study on the experimental parameters such as the thermal radiation from flame to atmospheric gas, the vessel cooling and the duration of sodium spill was performed. The results showed good agreements with experimental data in the literature.

1. Introduction

Liquid sodium is widely used as a coolant of LMR (Liquid Metal Reactor) because of its good physical and nuclear properties. However, liquid sodium spill will lead to sodium fire since the operating temperature of liquid sodium is above the ignition temperature. The sodium fire releases the heat from the chemical reaction with oxygen in the atmospheric gas and from the sensible heat of the spilled sodium. This can lead to containment failure due to the pressure increase in the containment vessel. Therefore the modeling of sodium fire plays an important role in the LMR safety analysis.

Beiriger et al. [1] has suggested that the burning rate of sodium pool fires in air is limited by the mass transport of oxygen to the burning zone. In his analytical model a thin vapor layer upon the surface of liquid pool was neglected and the flame temperature was assumed to be equal to the liquid surface temperature. The burning rate of his calculations would be too small since the actual flame temperatures are higher than that of the liquid sodium surface. On the other hand, Malet et al. [2] has suggested that the burning rate of sodium is proportional to the initial burning rate and depends on the oxygen concentration and the gas temperature. In the sodium pool fire, the initial burning rate depends on the geometrical and initial atmospheric gas conditions. The initial burning rate should be determined exactly to describe the sodium pool fire phenomena in his model.

This led some authors to carry out a theoretical study for clarifying the effect of the vapor layer on the burning rate of sodium pool fires. Newmann and Payne[3] and Kikuchi[4] have made the flame model to calculate the burning rate. Sodium vapor diffuses from the liquid sodium surface to the flame and then chemical reaction occurs in this flame region. In their models, however, the informations about the condition of atmospheric gas and behavior of reaction

products such as Na_2O and Na_2O_2, etc. are necessary to predict the sequence of sodium pool fire.

In this study, a sodium fire model is suggested to analyze the sodium pool fire in which both the flame and the reaction products are considered. And also a sodium pool fire analysis computer code, SOPA, is developed. The comparisons of the prediction results with the experimental data given in the literature were presented. The sensitivity studies of experimental parameters such as the thermal radiation from flame to atmospheric gas, the vessel cooling and the duration of sodium spill were performed. The results showed good agreements with experimental data in the literature.

2. Development of Mathematical Model

2.1. Physical Model and Basic Assumptions

In this sodium pool fire modeling, sodium vaporized from the liquid sodium surface by the heat transferred from the flame region. The sodium vapor diffuses toward the flame region where the chemical reaction of oxidation occurs. As shown in Fig. 1, the heat of chemical reaction is transferred from flame region to atmospheric gas, to wall structure and to sodium pool surface by radiation, convection and conduction.

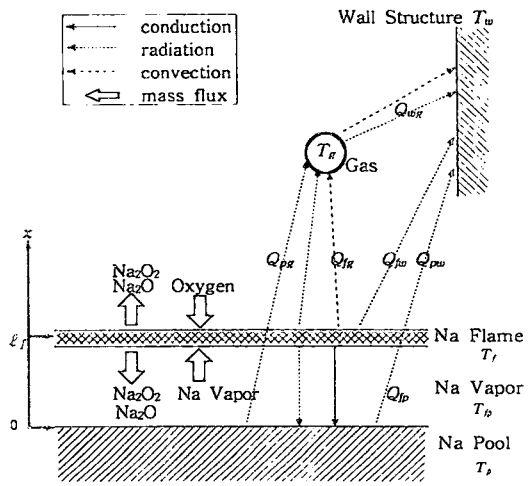

Fig. 1. Modeling of Sodium Pool Fire

For the modeling of burning rate, the following assumptions are made :

① Steady-state combustion is sustained under isobaric conditions,

② Entire heat is released from the flame surface of infinitesimal thickness where the weight fractions of sodium and oxygen approach zero,

③ The mass flow rates of sodium and oxygen are stoichiometric at combustion surface,

④ In the flame sheet, sodium and oxygen needed to sustain combustion are supplied by a diffusion mass flux from the pool and turbulent mass transfer from the atmospheric gas, respectively, and

⑤ The atmospheric gas obeys the ideal gas law.

2.2. Mathematical Model

2.2.1. Mass Balance at the Flame Sheet

Sodium Vapor Flux at the Flame Sheet

The diffusion equation of sodium vapor from the sodium surface to the flame sheet is given by[5]

$$C_f D_{Na} \frac{dY_{Na}(x)}{dx} = (\Phi_{Na} + \Phi_{N_2}) Y_{Na}(x) - \Phi_{Na} \qquad (1)$$

In Eq.(1), the inert gas flux, Φ_{N_2}, can be set to zero over the region between the flame and the pool surface since there is no sink for the inert gas. Equation (1) can be solved under the boundary condition at the pool surface.

$$Y_{Na}(x) = \frac{P_{Na,s}}{P_g} \qquad at\ x = 0 \qquad (2)$$

By integrating Eq.(1) and using the boundary condition of Eq.(2), $Y_{Na}(x)$ can be expressed as

$$Y_{Na}(x) = 1 - \left[\frac{P_g - P_{Na,s}}{P_g}\right] \cdot \exp\left(\frac{\Phi_{Na}}{C_f D_{Na}} \cdot x\right) \qquad (3)$$

At the flame, Y_{Na} becomes zero. Thus the sodium vapor flux at the flame sheet can be expressed as

$$\Phi_{Na} = \frac{C_f D_{Na}}{\ell_f} \cdot \ln\left[\frac{P_g}{P_g - P_{Na,s}}\right] \qquad (4)$$

By substituting Φ_{Na} into Eq.(3), the mole fraction of sodium vapor is obtained as follows:

$$Y_{Na}(x) = 1 - \left[\frac{P_g - P_{Na,s}}{P_g}\right]^{\left(1-\frac{x}{\ell_f}\right)} \quad (5)$$

Oxygen Mass Flux at the Flame Sheet

The equation for the oxygen mass transfer from the atmospheric gas to the flame sheet is expressed as[5]

$$\Phi_{O_2} = Y_{O_2}(\Phi_{O_2} + \Phi_{N_2}) + K \cdot (Y_{O_2} - Y_{O_2,f}) \quad (6)$$

where Y_{O2} and $Y_{O2,f}$ are the mole fraction of oxygen at the atmospheric gas and at the flame sheet, respectively.

Since there is no sink for inert gas at the flame sheet, Φ_{N2} becomes zero in Eq.(6). It was observed that in a combustion process, the chemical reaction rate is much higher than that of mass transfer process, so that $Y_{O2,f}$ can be set to zero. With these conditions, Φ_{O2} in Eq.(6) is transformed into

$$\Phi_{O_2} = \frac{Y_{O_2}}{1 - Y_{O_2}} \cdot K \quad at\ x = \ell_f \quad (7)$$

To obtain the mass transfer coefficient K in Eq.(7), the heat-mass transfer analogy is invoked[5]. The Fujii-Imura[6] empirical correlation for heat transfer from a heated horizontal plate to atmosphere was adapted to simulate the mass transfer of oxygen from the atmospheric gas to the flame sheet. The equation is:

$$Nu = 0.16\,(Gr \cdot \Pr)^{1/3} \quad \text{for } Gr \cdot \Pr < 2.0 \times 10^8 \quad (8)$$

By means of heat-mass transfer analogy, Eq.(8) becomes

$$Sh = 0.16\,(Gr \cdot Sc)^{1/3} \quad (9)$$

where *Sh*, *Gr* and *Sc* represent Sherwood number, Grashof number and Schmidt number, respectively. From Eqs.(7) and (9), the oxygen mass flux at the flame can be obtained as follows:

$$\Phi_{O_2} = 0.16\, D_{O_2}\left[g\frac{\beta_g}{\nu_g^2}\,(T_f - T_g)\,Sc\right]^{1/3} \cdot C_a \frac{Y_{O_2}}{1 - Y_{O_2}} \quad (10)$$

Mass Balance of Sodium Vapor at the Flame Sheet

If we introduce the proportional constant X, which is the stoichiometric combustion ratio, we can develop the mass balance of sodium vapor at the flame sheet conveniently.

$$X = \frac{\Phi_{Na}}{\Phi_{O_2}} \quad (11)$$

By substituting Eq.(4) and Eq.(10) into Eq.(11), the mass balance at the flame sheet is expressed as

$$\frac{C_f D_{Na}}{\ell_f} \cdot \ln\left(\frac{P_g}{P_g - P_{Na,s}}\right) = 0.16\, D_{O_2}\left[g\frac{\beta_g}{\nu_g^2}\,(T_f - T_g)\,Sc\right]^{1/3} \cdot \left(C_a \frac{Y_{O_2}}{1 - Y_{O_2}}\right) X \quad (12)$$

2.2.2. Energy Balance at the Flame Sheet

At the flame sheet, the heat flux of combustion $\ddot{Q}_b$ can be expressed as

$$\ddot{Q}_b = \ddot{Q}_{fg} + \ddot{Q}_{fp} + \ddot{Q}_{fw} \quad (13)$$

where

- $\ddot{Q}_b$ = heat flux of combustion
- $\ddot{Q}_{fg}$ = heat flux from the flame sheet to the atmospheric gas by convection and radiation
- $\ddot{Q}_{fp}$ = heat flux from the flame sheet to the sodium pool surface by conduction and radiation
- $\ddot{Q}_{fw}$ = heat flux from the flame sheet to the wall structure

The correlations of these $\ddot{Q}_b$, $\ddot{Q}_{fg}$, $\ddot{Q}_{fp}$ and $\ddot{Q}_{fw}$ can be written as follows:

$$\ddot{Q}_b = \Phi_{Na} \cdot M_{Na} \cdot Q \quad (= \Phi_{O_2} \cdot X \cdot M_{Na} \cdot Q) \quad (14.a)$$

$$\ddot{Q}_{fg} = h_{fg} \cdot (T_f - T_g) + \varepsilon_{fg}\,\sigma\,(T_f^4 - T_g^4) \quad (14.b)$$

$$\ddot{Q}_{fp} = \lambda_{N_2} \cdot \frac{dT_{fp}}{dx}\Big|_{x=\ell_f} + \varepsilon_{fp} \cdot \sigma \cdot (T_f^4 - T_p^4) \quad (14.c)$$

$$\ddot{Q}_{fw} = \sum_i \varepsilon_{fwi} \cdot \sigma \cdot (T_f^4 - T_{wi}^4) \quad (14.d)$$

where

- Q = combustion heat per unit mass of sodium

M_{Na} = mole flux of sodium

h_{fg} = convective heat transfer coefficient from the flame sheet to the atmospheric gas

The conductive heat flux from flame sheet to sodium pool surface can be obtained by solving Eq. (15).

$$\nabla \cdot ((Gc_p)_{eff} T_{fp} - \lambda_{eff} \nabla T_{fp}) = 0 \qquad (15)$$

$(Gc_p)_{eff}$ is the effective heat capacity related to mass transport and is defined as :

$$(Gc_p)_{eff} = (Gc_p)_{Na} - (Gc_p)_{Na_2O} - (Gc_p)_{Na_2O_2} \qquad (16)$$

where G is the mass flux in unit of kg/m^{2}sec. Therefore, Eq.(15) can be rewritten as

$$(Gc_p)_{eff} \cdot \frac{dT_{fp}}{dx} - \lambda_{eff} \cdot \frac{d^2T_{fp}}{dx^2} = 0 \qquad (17)$$

T_{fp} is the temperature of the region between the flame and the pool surface. The boundary conditions of T_{fp} are given as

$$T_{fp}(x) = T_f \quad at \ x = \ell_f$$

$$T_{fp}(x) = T_p \quad at \ x = 0$$

Also, the effective thermal conductivity in the vapor region(λ_{eff}) can be approximated as the thermal conductivity of nitrogen(λ_{N_2}), because $Y_{Na} \cdot \lambda_{Na}$ is much less than $Y_{N_2} \cdot \lambda_{N_2}$ in the sodium vapor region. With the boundary conditions and Eq.(17) the temperature distribution T_{fp} is obtained as

$$T_{fp}(x) = T_p + \frac{T_f - T_p}{\exp\left(\frac{(Gc_p)_{eff}}{\lambda_{N_2}} \ell_f\right) - 1} \cdot \left[\exp\left(\frac{(Gc_p)_{eff}}{\lambda_{N_2}} \cdot x\right) - 1\right] \qquad (18)$$

Using Eq.(18), we can obtain conductive heat flux as follows :

$$(Gc_p)_{eff} \lambda_{N_2} \frac{dT_{fp}}{dx} \Big|_{x=\ell_f} = \frac{(Gc_p)_{eff}(T_f - T_p)}{\exp\left[\frac{(Gc_p)_{eff} \cdot \ell_f}{\lambda_{N_2}}\right] - 1} \cdot \exp\left[\frac{(Gc_p)_{eff} \cdot \ell_f}{\lambda_{N_2}}\right] \qquad (19)$$

By substituting Eqs.(10) and (19) into Eqs.(14.a) and (14.c), respectively, and combining these with Eq.(14.b) and (14.d), the energy balance equation at the flame sheet is expressed as

$$0.16 D_{O_2} \left[g \frac{\beta_g}{\nu_g^2} (T_f - T_g) Sc\right]^{1/3} \left(C_a \frac{Y_{O_2}}{1 - Y_{O_2}}\right) \cdot X \cdot M_{Na} \cdot Q = 0.16 \lambda_g \left(g \frac{\beta_g}{\nu_g^2} \Pr\right)^{1/3} \cdot (T_f - T_g)^{4/3} + \varepsilon_{fg} \cdot \sigma \cdot (T_f^4 - T_g^4) + \frac{(Gc_p)_{eff}(T_f - T_p)}{\exp\left[\frac{(Gc_p)_{eff}}{\lambda_{N_2}} \ell_f\right] - 1} \cdot \exp\left[\frac{(Gc_p)_{eff}}{\lambda_{N_2}} \ell_f\right] + \varepsilon_{fp} \cdot \sigma \cdot (T_f^4 - T_p^4) + \sum_i \varepsilon_{fwi} \cdot \sigma \cdot (T_f^4 - T_{wi}^4) \qquad (20)$$

2.2.3. Energy Balance at the Pool

The energy equation for the pool is written as follows :

$$(m c_p)_{Na,i} \frac{dT_{p,i}}{dt} = \dot{Q}_{fp} - \dot{Q}_{pw} - \dot{Q}_{vap} + \dot{Q}_{i-1,i} - \dot{Q}_{i,i+1} \qquad (21)$$

where

$(mc_p)_{Na,i}$ = heat capacity in the ith node

T_{pi} = mean temperature of the sodium in the ith node

$\dot{Q}_{fp}$ = heat transfer rate from the flame sheet to the sodium pool surface by conduction and radiation

$\dot{Q}_{fw}$ = heat transfer rate from the pool surface to the wall structure by radiation

$\dot{Q}_{vap}$ = heat transfer rate of vaporization

$\dot{Q}_{i,i+1}$ = heat transfer rate by conduction between nodes ith and (i+1)th

The expressions of $\dot{Q}_{fp}$, $\dot{Q}_{fw}$, $\dot{Q}_{vap}$ and $\dot{Q}_{i,i+1}$ are as follows :

$$\dot{Q}_{fp} = \lambda_{N_2} \frac{dT_{fp}}{dx} \Big|_{x=0} \cdot A_p + \varepsilon_{fp} \cdot \sigma \cdot (T_f^4 - T_p^4) \cdot A_p \qquad (22.a)$$

$$\dot{Q}_{pw} = \sum_i \varepsilon_{pwg} \cdot \sigma \cdot (T_p^4 - T_{wi}^4) \cdot A_p \qquad (22.b)$$

$$\dot{Q}_{vap} = \Phi_{Na} \cdot M_{Na} \cdot \Delta H_v \cdot A_p \quad (22.c)$$

$$\dot{Q}_{i,i+1} = \lambda_{i,i+1} \cdot (T_i - T_{i+1}) \cdot A_{i,i+1} \quad (22.d)$$

$T_{p,i}$ can be defined as T_p in convenience. Using (18), we can obtain the heat flux by conduction at the pool surface as

$$\lambda_{N_2} \frac{dT_{fp}}{dx} \Big|_{x=0} = \frac{(G c_p)_{eff} (T_f - T_p)}{\exp\left[\frac{(G c_p)_{eff}}{\lambda_{N_2}} \ell_f\right] - 1} \quad (23)$$

The sodium pool temperature can be determined by solving Eq.(21) with the constitutive Eqs.(18) and (23).

2.2.4. Energy Balance at the Wall Structure

The energy equation is written as follows:

$$(m c_p)_{wi} \frac{dT_{wi}}{dt} = \dot{Q}_{fw} + \dot{Q}_{pw} - \dot{Q}_{wg} + \dot{Q}_{i-1,i} - \dot{Q}_{i,i+1} \quad (24)$$

where

- $(mc_p)_{wi}$ = heat capacity in the ith node
- T_{wi} = mean temperature of the structure in the ith node
- $\dot{Q}_{fw}$ = heat transfer rate from the flame sheet to the wall structure surface by radiation
- $\dot{Q}_{pw}$ = heat transfer rate from the pool surface to the wall structure by radiation
- $\dot{Q}_{wg}$ = heat transfer rate from the wall structure surface to the atmospheric gas by convection and radiation
- $\dot{Q}_{i,i+1}$ = heat transfer rate by conduction between nodes ith and (i+1)th

The expressions of $\dot{Q}_{fw}$, $\dot{Q}_{pw}$, $\dot{Q}_{wg}$ and $\dot{Q}_{i,i+1}$ are as follows:

$$\dot{Q}_{fw} = \varepsilon_{fw} \cdot \sigma \cdot (T_f^4 - T_w^4) \cdot A_p \quad (25.a)$$

$$\dot{Q}_{pw} = \varepsilon_{pw} \cdot \sigma \cdot (T_p^4 - T_w^4) \cdot A_p \quad (25.b)$$

$$\dot{Q}_{wg} = h_{wg} \cdot (T_w - T_g) \cdot A_p + \varepsilon_{wg} \cdot \sigma \cdot (T_w^4 - T_g^4) \cdot A_w \quad (25.c)$$

$$\dot{Q}_{i,i+1} = \lambda_{i,i+1} \cdot (T_{w,i} - T_{w,i+1}) \cdot A_{i,i+1} \quad (25.d)$$

2.2.5. Energy Balance at the Atmospheric Gas

The energy equation at the atmospheric gas is written as follows:

$$(m c_v)_g \frac{dT_g}{dt} = \dot{Q}_{fg} + \dot{Q}_{pg} + \dot{Q}_{wg} \quad (26)$$

where

- $(mc_v)_g$ = heat capacity of the atmospheric gas
- T_g = mean temperature of the atmospheric gas
- $\dot{Q}_{fg}$ = heat transfer rate from the flame sheet to the atmospheric gas by convection and radiation
- $\dot{Q}_{pg}$ = heat transfer rate from the pool surface to the atmospheric gas by radiation
- $\dot{Q}_{wg}$ = heat transfer rate from the wall structure to the atmospheric gas by convection and radiation

The expressions of $\dot{Q}_{fg}$, $\dot{Q}_{pg}$ and $\dot{Q}_{wg}$ are as follows:

$$\dot{Q}_{fg} = h_{fg}(T_f - T_g) \cdot A_p + \varepsilon_{fg} \cdot \sigma \cdot (T_f^4 - T_g^4) \cdot A_p \quad (27.a)$$

$$\dot{Q}_{pg} = \varepsilon_{pg} \cdot \sigma \cdot (T_p^4 - T_g^4) \cdot A_p \quad (27.b)$$

$$\dot{Q}_{wg} = h_{wg}(T_w - T_g) \cdot A_w + \varepsilon_{wg} \cdot \sigma \cdot (T_w^4 - T_g^4) \cdot A_w \quad (27.c)$$

2.2.6. Atmospheric Gas Pressure

The atmospheric gas is assumed to be ideal gas and the gas pressure is given by

$$P_g = C_a \cdot R \cdot T_g \quad (28)$$

2.2.7. Burning Rate, *BR(t)*

In this model, we can determine the six unknowns, ℓ_f, T_f, T_p, T_{wi}, T_g and P_g, by solving Eqs.(12),(20), (21),(24),(26) and (28) simultaneously along with the other equations which govern surrounding regions.

From the mass balance of sodium vapor at the flame sheet, the burning rate can be obtained as

$$BR(t) = \Phi_{Na} \cdot M_{Na}$$
$$= \Phi_{O_2} \cdot X \cdot M_{Na}$$
$$= 0.16\, D_{O_2}\left[g\frac{\beta_g}{\nu_g^2}(T_f - T_g)\cdot Sc\right]^{1/3}$$
$$\cdot X \cdot M_{Na} \cdot \frac{Y_{O_2}}{1-Y_{O_2}} C_a \quad (29)$$

2.3. Constitutive Equations

2.3.1. Stoichiometric Combustion Ratio(X) and Combustion Heat(Q)

The following chemical reactions occur during the combustion process in this model.

$$4\,Na + O_2 \rightarrow 2\,Na_2O + 4\,Q_1 \quad (30.a)$$

$$2\,Na + O_2 \rightarrow Na_2O_2 + 2\,Q_2 \quad (30.b)$$

If we introduce the factor f, which is the fraction of total oxygen consumed to form sodium monoxide, the above chemical reaction process is rewritten as

$$4f\,Na + f\,O_2 \rightarrow 2f\,Na_2O + 4f\,Q_1$$
$$2(1-f)Na + (1-f)O_2 \rightarrow (1-f)Na_2O_2 + 2(1-f)Q_2$$
$$\Rightarrow [4f + 2(1-f)]Na + O_2 \rightarrow 2f\,Na_2O$$
$$+ (1-f)Na_2O_2 + [4f\,Q_1 + 2(1-f)Q_2] \quad (31)$$

Therefore, we can express the X and Q with f, Q_1 and Q_2.

$$X = 2(1+f) \quad (32)$$

$$Q = \frac{2f\,Q_1 + (1-f)Q_2}{1+f} \quad (33)$$

2.3.2. Effective Heat Capacity Related to the Mass Transport

If we introduce the factor f_d, which is the fraction of total combustion products falling into the pool from the flame sheet, then

$$(G\,c_p)_{Na} = \Phi_{Na} \cdot M_{Na} \cdot c_{p\,Na} \quad (34.a)$$

$$(G\,c_p)_{Na_2O} = \left[\Phi_{Na}\frac{2f \cdot f_{d,Na_2O}}{2(1+f)}\right] \cdot M_{Na_2O} \cdot c_{p\,Na_2O}$$

$$(G\,c_p)_{Na_2O_2} = \left[\Phi_{Na}\frac{(1-f)f_{d,Na_2O_2}}{2(1+f)}\right] \cdot M_{Na_2O_2} \cdot c_{p\,Na_2O_2} \quad (34.c)$$

By using Eqs.(34.a) through (34.c) and Eq.(4), and by definition of effective heat capacity given in Eq. (17), the effective heat capacity can be expressed as

$$(G\,c_p)_{eff} = \frac{C_f D_{Na}}{\ell_f} \cdot \ln\left(\frac{P_g}{P_g - P_{Na,s}}\right) \cdot$$
$$\left[(M\,c_p)_{Na} - \frac{f \cdot f_{d,Na_2O}}{(1+f)} \cdot (M\,c_p)_{Na_2O} + \frac{(1-f)\,f_{d,Na_2O_2}}{2(1+f)} \cdot (M\,c_p)_{Na_2O_2}\right] \quad (35)$$

2.3.3. Oxygen Concentration, C_{O_2}

The oxygen concentration is defined as

$$C_{O_2} = C_a \cdot Y_{O_2} \quad (36)$$

where C_a and Y_{O_2} are total molar concentration of atmospheric gas and molar fraction of oxygen, respectively. The balance of oxygen concentration is given by

$$V_g \frac{dC_{O_2}}{dt} = -(\Phi_{O_2} \cdot A_p) \quad (37)$$

By definition, the molar fraction of oxygen is given by

$$Y_{O_2} = \frac{C_{O_2}}{C_{O_2} + C_{N_2}} \quad (38)$$

With Eq.(10), Eq.(37) is transformed into

$$\frac{dC_{O_2}}{dt} = -0.16\, D_{O_2} \cdot \left[g\frac{\beta_g}{\nu_g^2}(T_f - T_g)\cdot Sc\right]^{1/3} \cdot \frac{A_p}{V_g} \cdot \frac{C_a Y_{O_2}}{1-Y_{O_2}} \quad (39)$$

Therefore, Eqs.(38) and (39) yield

$$\frac{dY_{O_2}}{dt} = -0.16\, D_{O_2} \cdot \left[g\frac{\beta_g}{\nu_g^2}(T_f - T_g)\cdot Sc\right]^{1/3} \cdot \frac{A_p}{V_g} \cdot Y_{O_2} \quad (40)$$

During the small time interval Δt, the physical properties and temperature of the gas and temperature of the flame can be approximated to be constant. Therefore, Eq.(40) can be expressed as

$$\frac{dY_{O_2}}{dt} = -\zeta \cdot Y_{O_2} \tag{41}$$

where

$$\zeta = 0.16 D_{O_2} \cdot \left[g \frac{\beta_g}{\nu_g^2} (T_f - T_g) \cdot Sc \right]^{1/3} \cdot \frac{A_p}{V_g} \tag{42}$$

The value of ζ is the function of the time, t, but is constant during Δt. As a results, by integrating Eq. (41) during time interval Δt, we can obtain molar fraction of oxygen as follows:

$$Y_{O_2}(t+\Delta t) = Y_{O_2}(t) \cdot e^{(-\zeta \Delta t)} \tag{43}$$

3. Results and Discussion

With the flame model, the SOPA(Sodium Pool Fire Analysis Code) computer program has been developed to simulate sodium pool fire, and its algorithm is shown in Fig. 2. SOFIRE-II code[1], which is developed in USAEC, does not include the flame model, but it is used to predict the sodium pool fire, generally. Therefore, in this study, the AB1 sodium pool fire test[7] performed by HEDL was simulated by SOPA and SOFIRE-II code, and the comparisons of prediction accuracy between two codes are carried out to verify the importance of the flame model. In the result SOPA agrees well with the experimental data rather than SOFIRE-II computer code. Also the FAUNA-5 test[8] performed by KfK was simulated by SOPA, and the sensitivity study on the radiation effect, the vessel cooling effect, and the effect of sodium spill duration was presented.

The test conditions for AB1 test are presented in Table 1 and the calculation results are shown in Fig. 3. The predictions of atmospheric gas temperature and pressure are overestimated as compared to the experimental data, but the predictions of SOPA are more realistic than those of SOFIRE-II. At the beginning of test, the first peaks of temperature and pressure have been observed and it seems to be the effect of the sodium filling. During the sodium spill, the contact area between liquid sodium and atmospheric gas is larger than that after sodium spill and thus the sodium burning rate is much larger at the beginning.

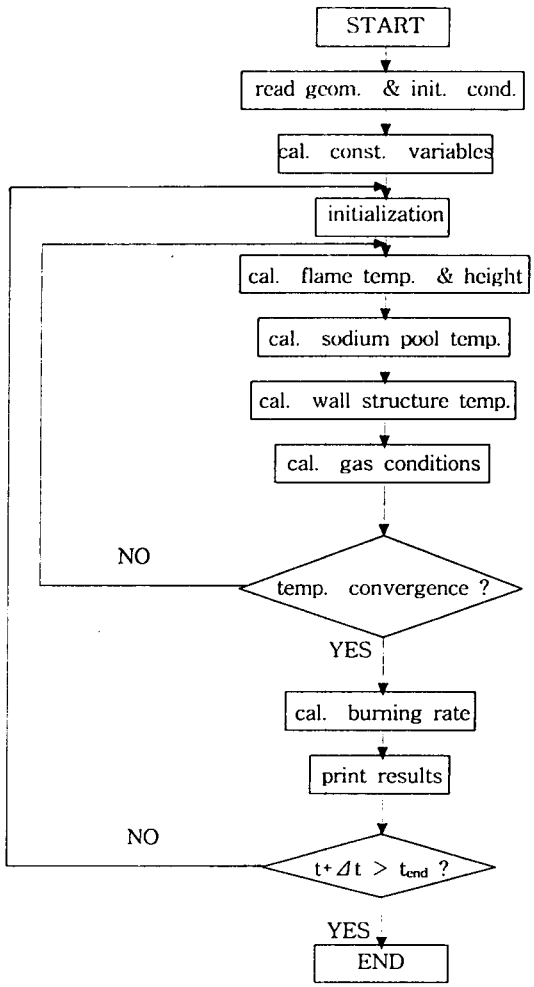

Fig. 2. Algorithm of the SOPA Computer Program

The test conditions for FAUNA-5 are shown in Table 2 and the calculation results are shown in Figs. 4 through 7. As shown in the figures, there is good agreement between the calculated results of SOPA in reference case and the experimental data. The con-

Table 1. Test Conditions for AB1 Test

Containment Vessel	
○ Diameter(m)	7.62
○ Overall height(m)	20.3
○ Volume(m^3)	850
○ Total internal surface(m^2)	1000
○ Leakage rate(%/day at 10 psig)	2.0
Sodium Spill	410
○ Mass sodium spill(kg)	4.4
○ Sodium burn pan surface(m^2)	600
○ Initial sodium temperature(℃)	60
○ Duration of sodium filling(s)	3600
○ Sodium fire duration(s)	
Initial Containment Atmosphere	
○ Oxygen(vol. %)	19.8
○ Temperature(℃)	26.5
○ Pressure(MPa, absolute)	0.125

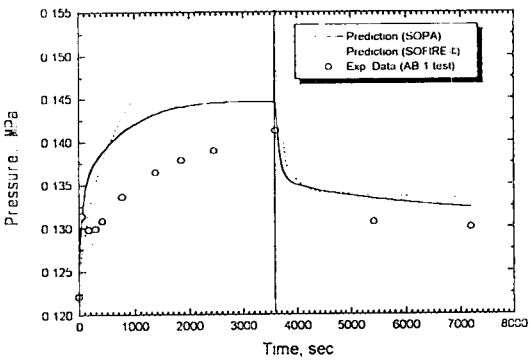

(a) Pressure of the Atmospheric Gas

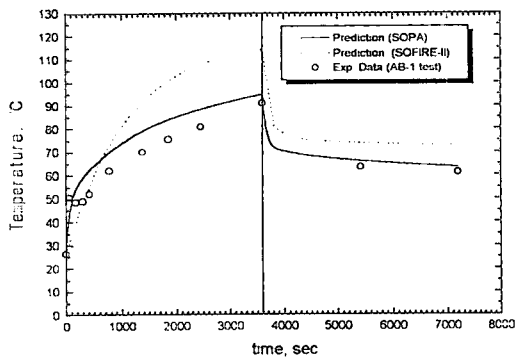

(b) Temperature of the Atmospheric Gas

Fig. 3. Comparison of Predicted and Experimental Data (AB-1 test)

ditions of reference case are ① with vessel cooling, ② without filling effect, and ③ $\varepsilon = 0.65$. As explained above, there are also first peaks in pressure and temperature of FAUNA-5 experimental data at the beginning of test. In Fig. 7, there is a temperature fluctuation in experimental data, and this phenomenon is also explained by the effect of sodium filling. This effect continues longer in case of the FAUNA-5 test than in the AB1 test because of the difference in sodium filling duration.

The sensitivity study on the effect of thermal radiation, vessel cooling and sodium spill duration was performed and shown in Figs. 4 through 7. In the figures, the solid line in the legend is the reference case, dashed line is the case of without vessel cooling, dot line is the case of with filling effect and centered line is the case of $\varepsilon = 0.3$. As shown in Figs. 4 and 7, there are great discrepancies between the cases with and without vessel cooling in the pressure and temperature of the atmospheric gas. In the case that the vessel cooling effect is not considered, the pressure in the vessel saturates to the maximum one and the temperature increases continuously. But in the case of vessel cooling, the pressure and temperature increase to the maximum value and decrease gradually. The maximum predicted pressure is the same in two cases, but the trend is greatly different. Therefore, the vessel cooling effect is important and it must be considered carefully in the sodium pool fire analysis.

In FAUNA-5 test, the sodium filling duration was 20 minutes. With filling effect, the contact area between liquid sodium and atmospheric gas is considered as 1.2 times of the burning pan area during first 20 minutes. In the early stage of test, the first peak pressure and temperature occur but the peak appearance time is faster than that of experiment. More detailed modeling about the sodium filling is required in SOPA program.

Lastly, the effect of thermal radiation from flame sheet to atmospheric gas is considered. The solid line is the case that the thermal radiation emissivity is

0.65 and the centered line is the case that the thermal radiation emissivity is 0.3. From these results, it is concluded that the effect of thermal radiation is less dominant than that of vessel cooling.

Table 2. Test Conditions for FAUNA-5 Test

test conditions	
Volume(m^3)	220
○ Wall area(m^2)	176
○ Wall thickness(mm)	16
○ Burning pan area(m^2)	2.0
○ Amount of sodium(kg)	350
○ Init. gas pressure(kg/cm^2 abs)	1.03
○ Init. gas/wall temperature(℃)	25
○ Init. sodium/pan temp.(℃)	480
○ Init. O_2 concentration(vol. %)	21
○ Duration of sodium filling(s)	1200
○ Sodium fire duration(s)	7200

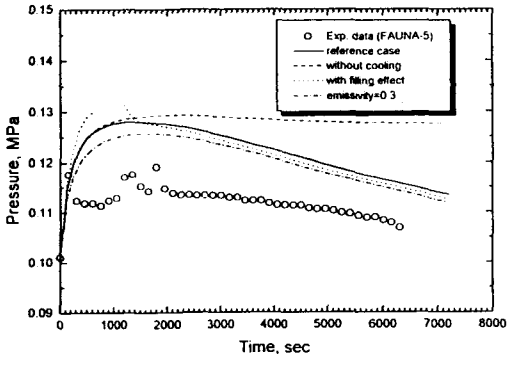

Fig. 4. Pressure of the Atmospheric Gas (reference case : with cooling, without filling effect and ε=0.65)

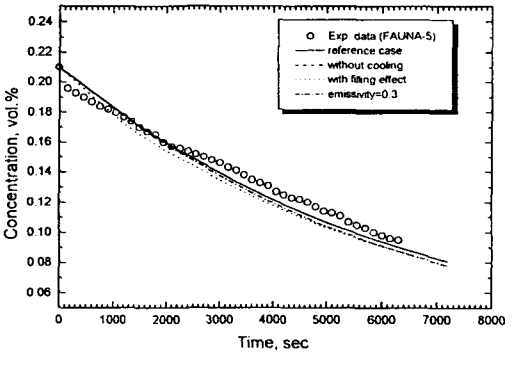

Fig. 5. Oxygen Concentration (reference case : with cooling, without filling effect and ε=0.65)

4. Conclusions

An advanced model is suggested to analyze the sodium pool fire where both the flame and the reaction products are considered. And also the SOPA computer program is developed. The numerical results showed good agreements with experimental data in the literature.

From the sensitivity study of experimental parameters such as the thermal radiation from flame to atmospheric gas, the vessel cooling and the duration of sodium spill, the following conclusions are obtained :

① since the vessel cooling effect shows the different trends in the temperature and pressure histories

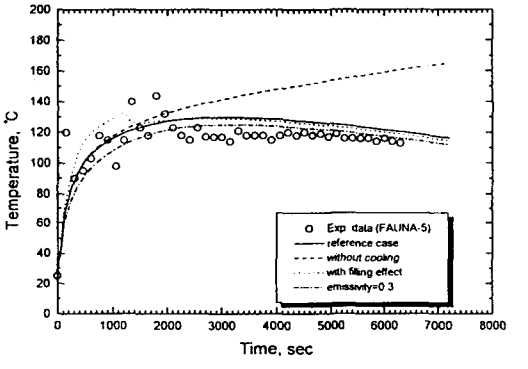

Fig. 6. Sodium Pool Temperature (reference case : with cooling, without filling effect and ε=0.65)

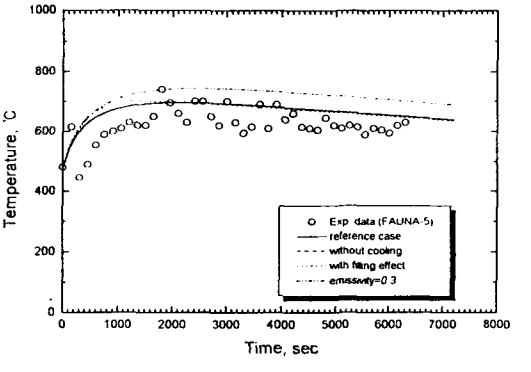

Fig. 7. Temperature of the Atmospheric Gas (reference case : with cooling, without filling effect and ε=0.65)

of the vessel, it must be considered carefully for the pool fire analysis,

② the sodium filling duration and condition are very sensitive in the early stage sodium pool fire, therefore the more detail model of the sodium filling mechanism is required in the future work, and

③ it is reasonable that the thermal radiation emissivity between the flame and the atmospheric gas is 0. 30-0. 65, but experimental verification is required.

Nomenclature

A area, m^2

C_a total molar concentration of atmospheric gas, mol-gas/m^3

C_f total molar concentration of gas in region between flame and pool, mol-gas/m^3

c_p specific heat at constant pressure, J/kgK

c_v specific heat at constant volume, J/kgK

D diffusion coefficient, m^2/sec

fraction of total consumed oxygen used to form sodium monoxide

g gravitational acceleration, m/sec^2

G mass flux, kg/m^2sec

h heat transfer coefficient, watt/m^2K

k mass transfer coefficient, m/sec

K mass transfer coefficient ($=C_a k$), mol/m^2sec

l distance between pool surface and flame zone, m

L reference length, m

m mass, kg

M molecular weight, kg/mol

$(Gc_p)_{eff}$ effective heat capacity related to mass transport, watt/m^2K

P pressure, Pa

Q combustion heat per unit mass, J/kg

$\dot{Q}$ heat transfer rate, watt

$\ddot{Q}$ heat flux, watt/m^2

T temperature, K

x distance from sodium pool surface, m

Y mole fraction

V_g volume of cell, m^3

Dimensionless Number

$$Gr = g\frac{\beta}{\nu^2}L^3\Delta T$$

$$Nu = \frac{hL}{\lambda}$$

$$Pr = \frac{\nu}{\alpha}$$

$$Sc = \frac{\nu}{D}$$

$$Sh = \frac{kL}{D}$$

Greek

α = thermal diffusivity, m^2/sec

β = volumetric thermal expansion coefficient, /K

ε = emissivity

λ = thermal conductivity, watt/mK

ν = kinematic viscosity, m^2/sec

σ = Stefan-Boltzmann constant, watt/m^2K^4

ζ = time averaged constant defined as Eq.(42), /sec

X = stoichiometric combustion ratio, mol-Na/mol-O_2

Φ = mole flux, mol/m^2sec

Subscript

1 monoxide formation

2 proxide formation

f flame

fg between flame and atmospheric gas

fp between flame and sodium pool

fw between flame and wall structure

g atmospheric gas

i i-th node

N_2 nitrogen

Na sodium

Na_s saturated sodium

O_2 oxygen

p sodium pool
pw between sodium pool and wall structure
vap vaporization of sodium
w wall structure

References

1. P. Beiriger, et al., "SOFIRE-II User Report," AI-AEC-13055 (1973)
2. J. C. Malet, et al., "Potential Results of Spray and Pool Fires," *Nucl. Eng. & Des.* 68, pp. 195-206 (1981)
3. R. N. Newmann and J.F.B. Payne, "The Burning Rates of Pool Fires," *Combustion and Flame*, 33, 291-297 (1978)
4. Y. Kikuchi, "Investigation of Burning Rate of Sodium Pool Fires," *J. of Nucl. Sci. & Tech.*, 23[1], 83-85 (1986)
5. R. Bayron Bird, et al., *Transport Phenomena*, John Wiley & Sons Inc., New York (1960)
6. T. Fujii and H. Imura, "Natural-Convection Heat Transfer from a plate with Arbitrary Inclination," *Int. J. Heat Mass Transfer*, 15, 755 (1972)
7. R. K. Hilliard, et al., "Aerosol Behavior during Sodium Pool Fires in a Large Vessel-CSTF Tests AB1 and AB2," HEDL-TME 79-28 UC-79, 79 (1979).
8. W. Cherdron and S. Jordan, "Thermodynamic and Aerosol-Physical Consequences of Sodium Pool Fires," IWGFR Specialists' Meeting on Sodium Fires Design and Testing, Washington, U.S. A, May 24-28, 1982 (1982).